

Stimulation and Artifact-Free Extracellular Electrophysiological Recording of Cells in Suspension

Frank B. Myers, Oscar J. Abilez, Chris K. Zarins, and Luke P. Lee

Abstract—We have developed instrumentation which stimulates and records electrophysiological signals from populations of suspended cells in microfluidic channels. We are employing this instrumentation in a new approach to cell sorting and flow cytometry which distinguishes cells based on their electrophysiology. This label-free approach is ideal for applications where labeling or genetic modification of cells is undesirable, such as in purifying cells for tissue replacement therapies. Electrophysiology is a powerful indicator of phenotype for electrically-excitabile cells such as myocytes and neurons. However, extracellular field potential signals are notoriously weak and large stimulus artifacts can easily obscure these signals if care is not taken to suppress them. This is particularly true for suspended cells. Here, we describe a novel microelectrode configuration and the associated instrumentation for suppressing stimulus artifacts and faithfully recovering the extracellular field potential signal. We show that the device is capable of distinguishing cardiomyocytes from non-cardiomyocytes derived from the same stem cell population. Finally, we explain the relationship between extracellular field potentials and the more familiar transmembrane action potential signal, noting the physiologically important features of these signals.

Keywords—*electrophysiology-activated cell sorting (EPACS), instrumentation amplifier, stimulation, field potential, cardiomyocytes, stem cells*

I. INTRODUCTION

ONE of the major obstacles in translating stem cell biology into tissue replacement therapy is the establishment of effective techniques for purifying fully-differentiated cells from other cells which may hamper graft performance or lead to teratoma formation [1]. Conventional sorting and cytometry techniques for stem cells require exogenous labeling or genetic modification, neither of which is ideal for clinical applications. However, many of the cell populations relevant for therapy are electrically-excitabile (e.g. cardiomyocytes, neurons, skeletal muscle, and vascular smooth muscle), meaning they produce transmembrane ion currents in response to electrical stimulation. Electrophysiological recordings of these signals can provide rich phenotypic information non-invasively and without

Manuscript received April 15, 2011. This work was supported by a National Science Defense and Engineering Graduate (NDSEG) Research Fellowship (FBM), Stanford ARTS Fellowship (OJA), CIRM (CKZ), NIH HL089027 (CKZ), NSF 0735551 (CKZ), DARPA MF3 HR0011-06-10050 (LPL).

F.B. Myers and L.P. Lee are with the Department of Bioengineering, University of California, Berkeley, CA. (e-mail: lplee@berkeley.edu).

O.J. Abilez and C.K. Zarins are with the Departments of Bioengineering (OJA) and Surgery (OJA and CKZ), Stanford University, Stanford, CA.

labeling [2], [3].

II. BASIS OF FIELD POTENTIAL SIGNALS

The field potential (FP) is the ohmic potential drop in the resistive medium surrounding a cell arising from transmembrane ion currents during depolarization (Figure 1). This voltage signal can be detected with a nearby microelectrode. Transient changes in membrane permeability following excitation lead to various diffusive ion currents (primarily, Na^+ , K^+ , and Ca^{2+}) in and out of the cell. These permeability changes also cause characteristic shifts in the Goldman-Hodgkin-Katz potential across the cell membrane, giving rise to the so-called transmembrane action potential signal [4]. Different cell types express different combinations

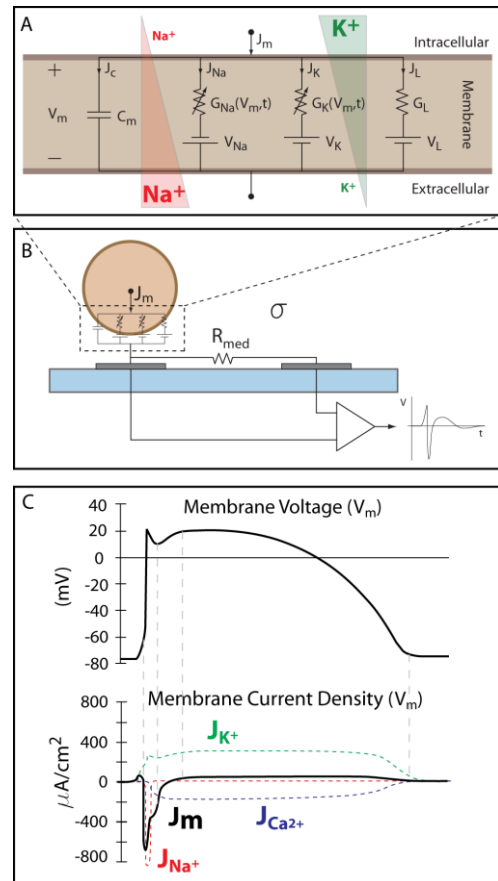


Fig. 1. (A) Hodgkin-Huxley model of membrane excitability. Na^+ and K^+ gradients primarily drive the depolarization/repolarization currents of electrically-excitabile cells. (B) field potentials arise due to ohmic drops from these currents in the vicinity of the cell. (C) relationship between transmembrane action potential and extracellular field potential.

III. INSTRUMENTATION

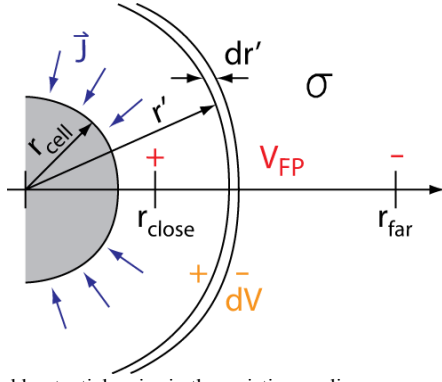


Fig. 2. Field potentials arise in the resistive medium surrounding a cell from the diffusive ion flux, J , entering/leaving the cell membrane.

of ion channels, which give them unique field potential or action potential signals. Thus, these signals are useful in assessing cell phenotype. Electrically, the transmembrane current density can be regarded as a capacitive charging current due to the changes in the Goldman-Hodgkin-Katz potential:

$$J_m = C_m \frac{dV_m}{dt}$$

where C_m is the specific capacitance of the cell membrane. The differential voltage, dV , across a spherical shell around the cell with resistance dR , is:

$$dV = 4\pi r_{cell}^2 J_m \cdot dR = I_m \cdot dR$$

where r_{cell} is the radius of the cell. Integrating this between two electrodes, one close to the cell and one far from the cell:

$$\begin{aligned} V_{FP} &= I_m \int_{r_{close}}^{r_{far}} \frac{1}{\sigma} \frac{dr'}{4\pi r'^2} \\ &= \frac{J_m r_{cell}}{\sigma} \left(\frac{r_{cell}}{r_{close}} - \frac{r_{cell}}{r_{far}} \right) \end{aligned}$$

where σ is the conductivity of the medium. Therefore, the field potential is related to the more familiar action potential (V_m) by:

$$V_{FP} = \frac{C_m r_{cell}}{\sigma} \left(\frac{r_{cell}}{r_{close}} - \frac{r_{cell}}{r_{far}} \right) \frac{dV_m}{dt}$$

Field potential recordings are often considered imprecise when compared with action potential signals. Field potential SNR is generally weaker than action potential SNR (as recorded with patch clamp techniques) and the cell positioning relative to the electrodes is difficult to precisely control. In our device, however, cell positioning is quite repeatable and electrode positions are precisely defined. Furthermore, microchannels confine the current distribution around the cell to a smaller volume, increasing the ohmic drop and enhancing the field potential signal. For these reasons, field potential signals recorded in microchannels can provide more quantitative physiological parameters than conventional microelectrode array (MEA) recordings.

Figure 3 shows our prototype cell sorter. Cells or cell clusters are introduced as a dilute suspension into a microfluidic device consisting of polydimethylsiloxane (PDMS) microchannels and platinum microelectrodes with contact pads around the perimeter of the device [5]. The channel has a $1000 \times 400 \mu\text{m}$ cross-section. Two large, rectangular stimulation electrodes ($200 \times 1000 \mu\text{m}$) are positioned just upstream and downstream of a pair of differential sensing electrodes ($40 \mu\text{m}$ diameter) separated by $200 \mu\text{m}$. Clusters of cells $\sim 200 \mu\text{m}$ in diameter are loaded into the device and positioned on top of one of these sensing electrodes. A custom printed circuit board (PCB) containing an instrumentation amplifier and an optoisolated, battery-powered stimulator is interfaced to the microfluidic chip via spring-loaded gold pins. The amplifier is configured with a gain of 60 dB. It consists of a FET-input instrumentation amplifier, followed by a sample and hold amplifier configured as a blanking circuit which prevents saturation of the downstream circuitry. This is followed by a two-stage op-amp bandpass filter with a passband of 4 Hz – 50 kHz. An NPN optoisolator with a bandwidth of 250 kHz is used to generate voltage-controlled current stimulus pulses from a battery. Although more sophisticated current sources can be used, it was found that the optoisolator alone delivers constant current pulses within the range of 100 μA – 5 mA

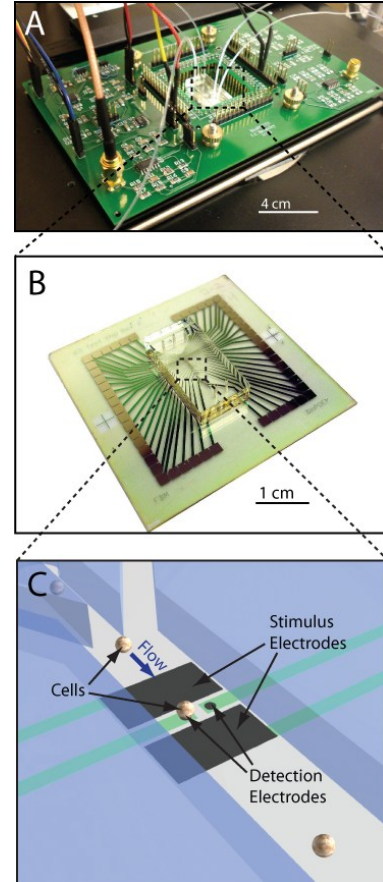


Fig. 3. (A) Prototype instrumentation and (B) microfluidic device for electrophysiology-activated cell sorter (EPACS). (C) 3D model of cells entering stimulation/detection region of microfluidic device.

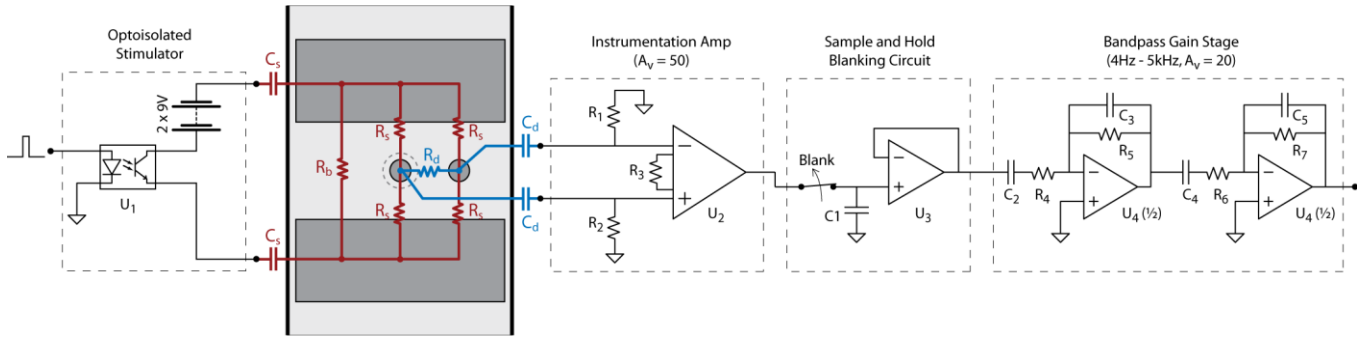


Fig. 4. Schematic showing a battery-powered optoisolated stimulator, electrical model of the stimulation and detection electrodes and channel resistances, and instrumentation amplifier. Table 1 lists component values.

into the impedance of our device (approximately 1 k Ω) with good linearity versus the applied voltage.

The entire system is enclosed in a Faraday cage to minimize interference. A glass slide coated with a thin film of indium tin oxide (ITO) is positioned underneath the device and a controlled DC current is delivered through the ITO which warms the device to 37 $^{\circ}$ C uniformly over the area of the chip. Closed-loop temperature feedback is provided by a thermistor connected to a bridge circuit.

Custom LabVIEW controller software in conjunction with a 16-bit data acquisition module (National Instruments, Austin, TX) is used to generate stimulus and blanking pulses and digitize signals from the device at a sampling rate of 100 kHz. An LCR meter (Model 4284A, Agilent, Santa Clara, CA) is used to monitor the impedance between the detection electrodes, and this information is continuously relayed to the LabVIEW controller via a GPIB bus. When a cell is detected, the LabVIEW controller turns off the LCR meter's interrogation signal and disconnects it from the detection electrodes via two analog switches. At that point, the stimulus pulse is delivered and the recorded signal from the instrumentation amplifier is processed. The LabVIEW controller also automates a syringe pump (PHD Ultra, Harvard Apparatus, Holliston, MA) for cell delivery, controls electromechanical valves which switch the outlet flow to one of several reservoirs (Pneumadyne, Plymouth, MN), and maintains the temperature by modulating the current through the ITO heater using a closed-loop proportional-integral-derivative (PID) controller.

IV. STIMULUS ARTIFACT SUPPRESSION

Typical extracellular electrophysiology experiments are performed with 2D tissue preparations. In those experiments, the requirements on artifact suppression are relaxed, because it's generally not necessary to measure signals from the same cell that is being directly stimulated, and due to propagation delay in the tissue, stimulation and field potential onset are temporally decoupled. Here, since we must stimulate and record from the same cells, careful consideration must be given to stimulus artifact suppression.

There are three modes by which the stimulus signal can couple into the detection circuitry and introduce artifact: ohmic voltage gradients, common-mode conversion, and direct capacitive coupling between the stimulus and recording electrodes [6]. To eliminate ohmic voltage

gradients between the recording electrodes, we employed a differential sensing scheme where electrodes are placed on an equipotential line between the stimulus electrodes, essentially forming a balanced bridge circuit (Figure 4). For our stimulus currents, this leads to voltage drops which are well below the thermal noise floor. Common-mode conversion is mitigated by the use of a high-impedance instrumentation amplifier (10^{12} Ω input impedance, 120 dB common mode rejection at 60 Hz) which does not share a common ground with the stimulator, preventing DC current from flowing from the stimulus electrodes into the recording amplifier. Capacitive coupling between the stimulus and recording leads is dramatically reduced by platinizing the electrodes [7], which increases the double layer capacitance of the sensing electrodes from 110 pF to 13.9 nF. Our amplifier employs a blanking circuit following the input stage which disconnects the downstream bandpass filter stage during stimulation. The blanking signal is generated simultaneously with the stimulus signal from a Labview PC

TABLE I
COMPONENT VALUES FOR AMPLIFIER

Symbol	Component	Description
U1	4N25	Optoisolator (NPN Output)
U2	INA121	FET-Input Instrumentation Amp
U3	LF398	Sample & Hold Amp
U4	OPA2130	Dual FET-Input Op-Amp
R1, R2	1 G Ω	Bias Current Return Resistors
R3	1 k Ω	Gain-Setting Resistor
R4, R6	18.2 k Ω	High-Pass Filter Resistor
R5, R7	90.9 k Ω	Low-Pass Filter Resistor
C1	10 nF	Hold Capacitor
C2, C4	2.2 μ F	High-Pass Filter Capacitor
C3, C5	330 pF	Low-Pass Filter Capacitor

TYPICAL MEASURED DEVICE IMPEDANCES (AT 1 KHZ)		
Rb	5 k Ω	Bulk Resistance
Rs	500 k Ω	Stim-to-Cell Resistance (est.)
Rd	10 k Ω	Resistance Between Detection Electrodes
Cs	180 nF	Stimulation Electrode Double-Layer Capacitance
Cd	30 nF	Detection Electrode Double-Layer Capacitance (w/Pt black)

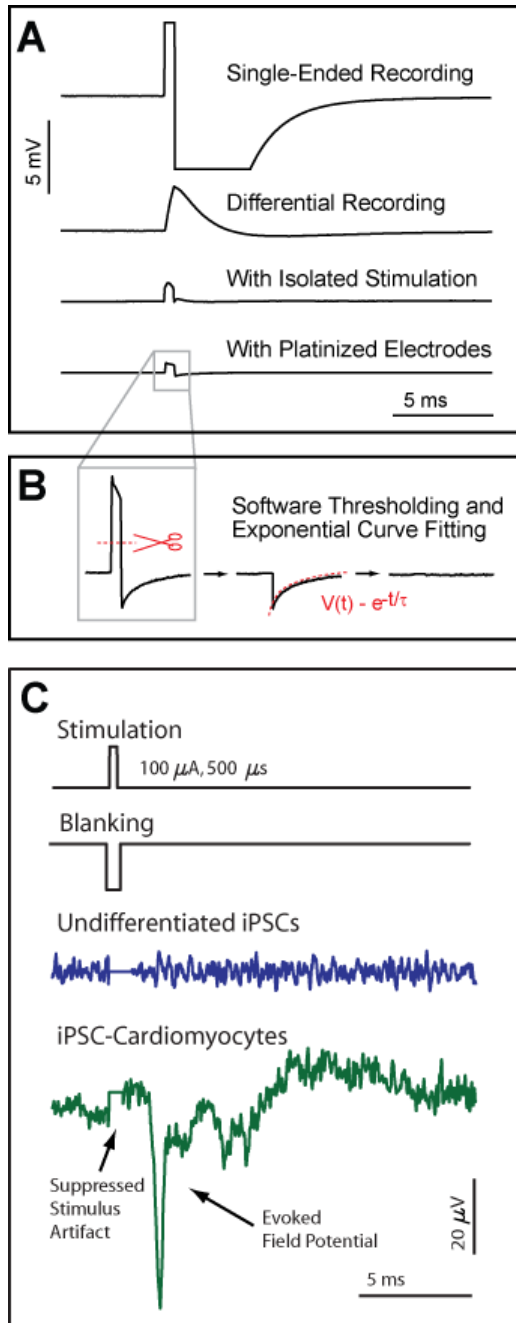


Fig. 5. (A-B) Artifact suppression is achieved through a combination of instrumentation, electrode placement, and software techniques. (C) Evoked field potentials are observed only from stem cells which have undergone cardiomyocyte differentiation.

controller. The remaining artifact for a typical 500 μs , 100 μA stimulus pulse is an exponential decay signal with peak amplitude <1 mV (input-referred). This is removed in software via least squares exponential curve fitting and subtraction.

V. MICROCHANNELS ENHANCE FIELD POTENTIALS

Although extracellular field potential signals are weak when compared to patch clamp signals, we have observed that when cells are confined to microchannels, the field potential amplitude increases substantially due to the confinement of current through the cross section of the channel. When cells

are confined to microchannels, the diffusive ion flux through the membrane, and therefore the current through the medium, is essentially the same as when they are on a planar substrate, but the resistance through which that current must travel scales inversely with the channel's cross-sectional area, leading to higher field potential amplitudes.

VI. RESULTS

Figure 5A compares stimulus artifacts in our device for a single-ended recording (vs. Ag/AgCl reference) versus differential recording using our symmetric electrode structure. Further improvements are made by isolating the stimulation circuit and platinizing the electrodes. The remaining artifact is removed in software via thresholding and exponential curve fitting, as illustrated in Figure 5B.

Figure 5C shows the result of stimulating undifferentiated induced pluripotent stem cell (iPSC) clusters and iPSC clusters which have been differentiated into cardiomyocytes using the Activin-A and BMP-4 growth factors [8]. A 500 μs stimulus current pulse is applied along with an amplifier blanking signal which is applied 200 μs before and after the stimulus pulse. A 200 μV field potential is evoked from the cardiomyocytes immediately following stimulation; no discernable response is seen from the undifferentiated cells. As clusters may themselves be heterogeneous, however, we are now developing a system with single cell resolution.

ACKNOWLEDGMENT

We would like to thank Josh Baugh and Madhu Gorrepati for help with cell culture, Kevin Pimentel for help with system construction, Patrick Goodwill for help with circuit design, and Paul Lum of the UC Berkeley Biomolecular Nanotechnology Center.

REFERENCES

- [1] E. M. Hansson, M. E. Lindsay, and K. R. Chien, "Regeneration Next: Toward Heart Stem Cell Therapeutics," *Cell Stem Cell*, vol. 5, no. 4, pp. 364-377, Oct. 2009.
- [2] K. Banach, M. D. Halbach, P. Hu, J. Hescheler, and U. Egert, "Development of electrical activity in cardiac myocyte aggregates derived from mouse embryonic stem cells," *Am J Physiol Heart Circ Physiol*, vol. 284, no. 6, pp. H2114-2123, Jun. 2003.
- [3] C. Mummery et al., "Differentiation of human embryonic stem cells to cardiomyocytes: role of coculture with visceral endoderm-like cells," *Circulation*, vol. 107, no. 21, pp. 2733-2740, Jun. 2003.
- [4] T. F. Weiss, *Cellular Biophysics, Vol. 2: Electrical Properties*. The MIT Press, 1996.
- [5] F. B. Myers, O. J. Abilez, C. K. Zarins, and L. P. Lee, "Electrophysiological Sorting of Pluripotent Stem Cell-Derived Cardiomyocytes in a Microfluidic Platform," presented at the 14th International Conference on Miniaturized Systems for Chemistry and Life Sciences (MicroTAS), Groningen, Netherlands, 2010, pp. 893-895.
- [6] K. C. McGill et al., "On the Nature and Elimination of Stimulus Artifact in Nerve Signals Evoked and Recorded Using Surface Electrodes," *Biomedical Engineering, IEEE Transactions on*, vol. 29, no. 2, pp. 129-137, 1982.
- [7] D. Malleo, J. T. Nevill, A. van Ooyen, U. Schnakenberg, L. P. Lee, and H. Morgan, "Note: Characterization of electrode materials for dielectric spectroscopy," *Review of Scientific Instruments*, vol. 81, no. 1, p. 016104, 2010.
- [8] M. A. Laflamme et al., "Cardiomyocytes derived from human embryonic stem cells in pro-survival factors enhance function of infarcted rat hearts," *Nat Biotech*, vol. 25, no. 9, pp. 1015-1024, 2007.